2012 International Conference on Lightning Protection (ICLP), Vienna, Austria

Analysis of NLDN-estimated peak currents for positive cloud-to-ground lightning

Amitabh Nag[1], Vladimir A. Rakov
Department of Electrical and Computer Engineering,
University of Florida, Gainesville, Florida, USA
[1] Now at Vaisala Inc., Tucson, Arizona, USA

Kenneth L. Cummins
Department of Atmospheric Sciences
University of Arizona
Tucson, Arizona, USA

***Abstract*— We infer peak currents from radiation electric field peaks of 48 positive return strokes acquired at the Lightning Observatory in Gainesville (LOG), Florida, in 2007-2008. In doing so, we use the transmission line model, NLDN-reported distances, and assumed return-stroke speed. From a similar analysis of negative first and subsequent strokes, it appears that the implied return-stroke speed in the NLDN field-to-current conversion equation is 1.8 x 10^8 m/s. The NLDN uses the same field-to-current conversion procedure (and hence the same implied return-stroke speed) for positive return strokes. However, for positive return strokes and an assumed return stroke speed of 1.8 x 10^8 m/s, NLDN-reported peak currents are not consistent with the transmission line model predicted peak currents (differ by 27% on average). The discrepancy between regression equations for negative first and subsequent strokes on the one hand and positive return strokes on the other hand suggests that the NLDN procedure to compensate for field propagation effects and find the average range-normalized signal strength (RNSS) works differently for these two groups of strokes. We find that the difference can be explained by the bias towards NLDN sensor reports from larger distances for positive strokes combined with the higher relative sensor gain at larger distances.**

Keywords- positive lightning; NLDN; peak current

I. INTRODUCTION

Due to their relative paucity, positive lightning discharges are considerably less studied and understood than their negative counterparts. The charge structure and evolution of thunderclouds that produce positive lightning, as well as in-cloud processes that can lead to its initiation, largely remain a mystery. Nag and Rakov (2012) [1] examined the various conceptual cloud charge configurations and scenarios leading to production of positive lightning discharges. Further, they examined various features of positive cloud-to-ground lightning discharges such as multiplicity, preliminary breakdown, leader stepping, charge transfer, and occurrence within otherwise negative cloud-to-ground flashes (which constitutes a bipolar flash). Data for 52 positive cloud-to-ground flashes containing 63 strokes recorded at the Lightning Observatory in Gainesville (LOG), Florida, in 2007–2008 were presented and discussed. The U.S. National Lightning Detection Network (NLDN) located 51 (96%) of the positive strokes of which 48 (91%) were correctly identified and 3 positive return strokes were misidentified as cloud discharges.

In this paper, we use the transmission line model (Uman and McLain, 1969 [2]) to infer peak currents from measured radiation electric field peaks for these 48 positive return strokes, NLDN reported distances, and assumed return-stroke speed and compare them with those reported by the NLDN. Further, we compare the results to those for negative lightning and discuss the observed differences.

II. EXPERIMENTAL SETUP AND DATA

As noted in Section I, the data presented here were acquired at the LOG located on the University of Florida campus in Gainesville, Florida. The LOG includes instrumentation to measure electric field and electric field derivative (dE/dt) waveforms. The electric field sensor consisted of a circular flat-plate antenna followed by an integrator and a unity gain, high-input-impedance amplifier. The system had a useful frequency bandwidth of 16 Hz to 10 MHz, the lower and upper limits being determined by the RC time constant (about 10 ms) of the integrator and by the amplifier, respectively. The electric field derivative (dE/dt) measuring system included a circular flat-plate antenna followed by an amplifier. The upper limit of frequency bandwidth of the dE/dt measurement was 17 MHz. Fiber optic links were used to transmit the signals from the antennas and associated electronics to an 8-bit digitizing oscilloscope. The oscilloscope digitized the signals at 100 MHz and recorded them in its memory unit. The record length was either 240 ms with a pretrigger of 80 ms or 500 ms with a pretrigger of 100 ms. The calibration of the electric field and electric field derivative measuring systems is discussed by Nag (2010) [3] and Nag et al. (2010) [4]. In particular, the presence of the building on which the antennas were placed was accounted for using FDTD calculations of Baba and Rakov (2007) [5]. The electric field measurement errors are discussed in detail by Nag et al. (2010, Appendix A1) [4].

NLDN-reported distances from the field measuring station for the 48 correctly identified positive strokes (in 40 flashes) ranged from 7.8 to 157 km and for 3 misidentified strokes from 1.8 to 5 km. The majority (31 out of the 48) of strokes were within 60 km of LOG, with 6, 14, 11, and 17 occurring in the 5–20, 20–40, 40–60, and 60–160 km ranges, respectively.

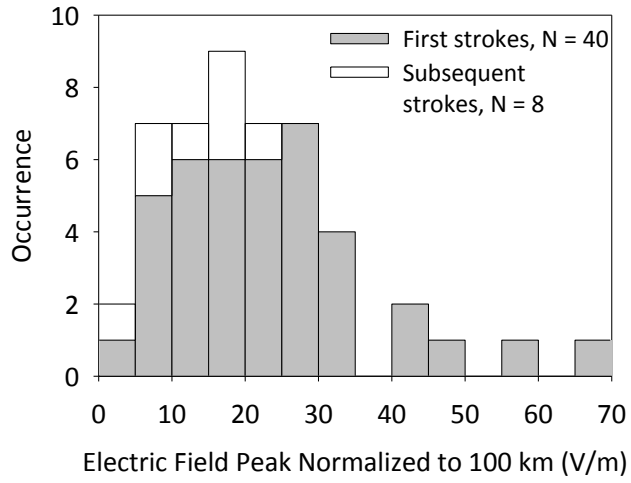

	First return strokes	Subsequent return strokes	All
AM, V/m	23.4	13.2	21.7
GM, V/m	19.8	11.7	18.1
Min, V/m	5.0	4.34	4.34
Max, V/m	66.3	20.3	66.3
N	40	8	48

Figure 1. Histogram of the initial electric field peak normalized to 100 km for 48 positive return strokes. Statistics given are arithmetic mean (AM), geometric mean (GM), minimum (Min), and maximum (Max) values for first and subsequent strokes, as well as for all data combined.

III. ANALYSIS

A. Distance-Normalized Electric Field Peak

The electric field change due to a positive return stroke is negative according to the atmospheric electricity sign convention. Only the magnitude of the electric field change is considered here.

The measured initial electric field peak normalized to 100 km for 48 positive return strokes located at distances of 7.8 to 157 km ranged from 4.34 to 66.3 V/m. The arithmetic mean (AM) and geometric mean (GM) field peaks were 21.7 V/m and 18.1 V/m, respectively. The histogram of the initial electric field peak normalized to 100 km for the 48 return strokes is shown in Figure 1. Note that the GM normalized initial peak for 8 subsequent strokes (11.7 V/m) is appreciably lower than that for 40 first strokes (19.8 V/m). Number of strokes in different distance ranges and corresponding GM values of field peaks normalized to 100 km are given in Table I.

B. Peak Current Estimated by the NLDN

The NLDN outputs a peak current estimate for each stroke using the measured magnetic radiation field peaks and distances to the ground strike point reported by multiple sensors. The following empirical field-to-current conversion equation is used:

$$i_p = 0.185\ \mathrm{Mean(RNSS)} \quad (1)$$

where i_p is the peak current in kA and Mean(RNSS) is the arithmetic mean of range–normalized (to 100 km) magnetic field signal strengths, in so-called LLP units, from all sensors allowed by the central analyzer to participate in the peak current estimate. Generally, contributions from sensors at distances up to several hundreds of kilometers are included. Equation 1 implies that the magnetic (as well as electric) radiation field is proportional to the current.

Normalization of measured magnetic field signal strength, SS, to 100 km is performed taking into account signal attenuation due to its propagation over lossy ground. The following empirical formula has been used since 2004 to compensate for the field propagation effects (Cummins et al., 2006 [6]):

$$RNSS = SS(\frac{r}{100})\exp(\frac{r-100}{1000}) \quad (2)$$

where r is in kilometers and SS is in LLP units. This equation assumes that the distance dependence of signal strength is $r^{-1}\exp(\frac{-r}{1000})$, where r^{-1} corresponds to propagation over perfectly conducting ground and $\exp(\frac{-r}{1000})$ represents additional attenuation due to ground being lossy. The exponential function in Equation 2 should increase the RNSS in order to compensate for propagation effects. For r = 625 km, for example, this function is equal to 1.7, although no compensation is provided for r = 100 km and for r ranging from 0 to 100 km it varies from about 0.9 to 1.

The median value of absolute current estimation error by the NLDN for negative subsequent strokes was found, using rocket-triggered lightning data, to be about 13% (Nag et al., 2011 [7]).

The distribution of the NLDN-estimated peak currents for 48 positive return strokes (in 40 flashes) occurring at distances ranging from 7.8 to 157 km is shown in Figure 2. The peak currents range from 19.8 to 234 kA with the AM and GM being 87.8 kA and 74.6 kA, respectively. For 40 first strokes, the AM and GM peak currents were 93.4 kA and 78.9 kA, respectively, and for 8 subsequent strokes the AM and GM values were 59.5 kA and 56.4 kA, respectively. Even though the minimum NLDN-estimated peak current tends to increase with distance, the dependence of the NLDN-estimated peak current on distance for the sample of 48 positive return strokes is rather weak (determination coefficient = 0.27). Table II gives the number of recorded strokes in different distance ranges along with the GM NLDN-estimated peak current for each distance range. The GM peak current generally increases with increasing distance which suggests a bias in the sample of 48 positive return strokes toward higher-intensity events, recorded from larger distances. Note that even for distances less than 20 km the GM peak current is higher than for negative return strokes (Rakov and Uman, 2003 [8]).

TABLE I. NUMBER OF POSITIVE STROKES IN DIFFERENT DISTANCE RANGES AND CORRESPONDING GM ELECTRIC FIELD PEAKS NORMALIZED TO 100 KM.

Distance range, km	**5-20**	**20-40**	**40-60**	**60-80**	**80-100**	**100-160**	**0-160**
Number of events	6	14	11	4	5	8	48
GM electric field peak normalized to 100 km, V/m	10.8	17.3	14.4	23.8	23.0	30.1	18.1

TABLE II. NUMBER OF POSITIVE RETURN STROKES (40 FIRST AND 8 SUBSEQUENT) IN DIFFERENT DISTANCE RANGES AND CORRESPONDING GM NLDN-ESTIMATED PEAK CURRENTS.

Distance range, km	**5-20**	**20-40**	**40-60**	**60-80**	**80-100**	**100-160**	**0-160**
Number of events	6	14	11	4	5	8	48
GM NLDN-estimated peak current, kA	45	61	66	119	96	124	75

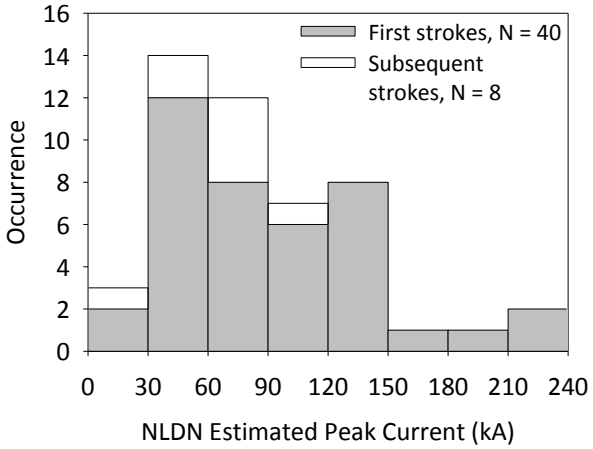

	First return stroke	**Subsequent return stroke**	**All**
AM, A	93.4	59.5	87.8
GM, A	78.9	56.4	74.6
Min, A	19.8	28.2	19.8
Max, A	234	91.6	234
N	40	8	48

Figure 2. Histogram of the NLDN-estimated peak currents for 48 positive return strokes. Statistics given are arithmetic mean (AM), geometric mean (GM), minimum (min), and maximum (max) values for first and subsequent strokes, as well as for all data combined.

C. Linear Regression Equations Relating NLDN Currents and Distance-Normalized Fields

As noted earlier, according to the atmospheric electricity sign convention, for positive return strokes the electric field change is negative. The corresponding current is assumed here to be positive. The scatter plot of the NLDN-estimated peak current I_{NLDN} versus electric field peak normalized to100 km E is shown in Figure 3. The two parameters appear to be linearly correlated (determination coefficient = 0.85), with the linear regression equation being given by:

$$I_{NLDN} = 11.3 - 3.5E \quad (3)$$

where E is negative and in V/m and I_{NLDN} is positive in kA.

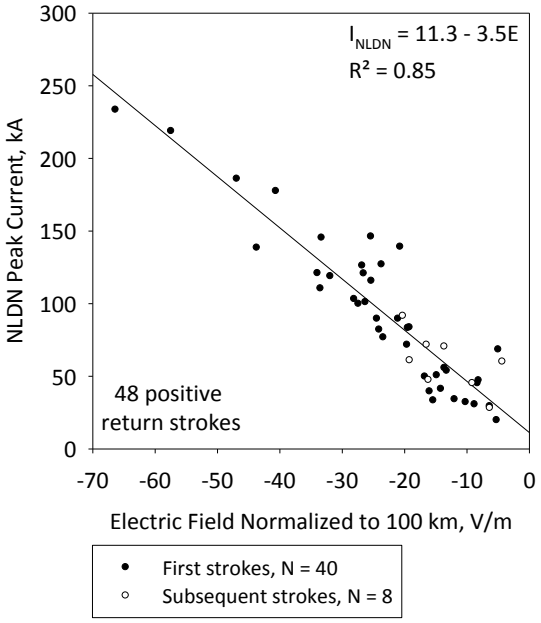

Figure 3. NLDN-estimated peak current versus normalized electric field peak for 48 positive return strokes. Also shown is the regression line.

Rakov et al. (1992b) [9] used the electric fields measured at 5 km and directly measured currents for 28 negative triggered-lightning strokes published by Willett et al. (1989) [10] to derive a regression equation that relates the negative subsequent return-stroke peak current I to the corresponding peak electric field E at distance D:

$$I = 1.5 - 0.037ED \quad (4)$$

where E is positive and in V/m, D is in kilometers, and I is negative and in kA. For D = 100 km, Equation 4 reduces to I = 1.5 - 3.7E. Pavlick et al. (2002) [11] used Equation 4 to estimate peak currents from the measured electric fields for 178 negative first return strokes occurring at distances ranging from 50 to 250 km. They found the NLDN-reported peak currents to be, on average, 10% lower than those estimated using Equation 4. Haddad et al. (2012) [12] found that the NLDN-reported peak current is on average about 20% lower than that predicted

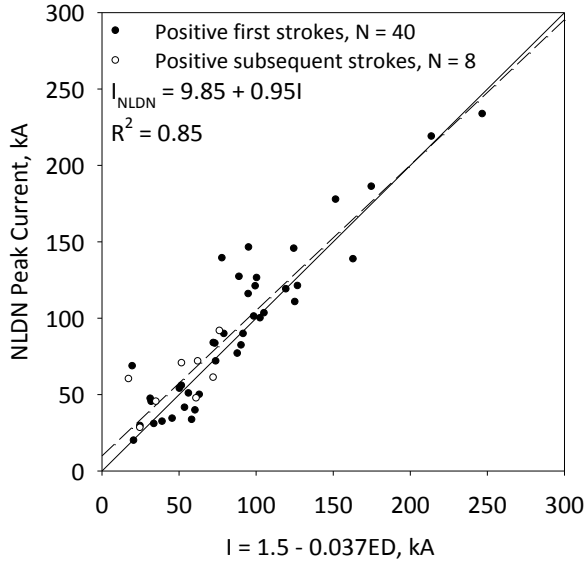

Figure 4. NLDN-estimated peak current versus peak current estimated using Equation 4 (with E being negative). The solid line is the diagonal with slope = 1 and the dashed line is the linear regression line.

by Equation 4 for the negative first strokes and about 26% lower for negative subsequent strokes. Note that while Equation 4 was derived using electric fields measured at 5 km from the return stroke channel, for both Pavlick et al. (2002) [11] and Haddad et al. (2012) [12] the electric fields used to estimate peak currents were measured at several tens to hundreds of kilometers from the channel.

Equation 4 (with E being negative) was formally applied here to estimate peak currents for 48 (40 first and 8 subsequent) positive return strokes from their measured electric field peaks. The scatter plot of the peak current estimated from Equation 4 versus NLDN-estimated peak current is shown in Figure 4. The slanted (diagonal) solid line (slope = 1) is the locus of points for which the regression-equation-estimated peak current and the NLDN-estimated peak current are equal. For the sample of 48 positive return strokes, the points are approximately evenly scattered around this line. Also shown is the linear regression line (dashed) having a slope of 0.95 and determination coefficient of 0.85. The NLDN-reported peak currents were found to be, on average, 16% greater than those estimated using Equation 4.

For comparison, we examined 116 negative return strokes that were recorded in August, 2008, during two thunderstorms in Gainesville, Florida, using the same instrumentation as that employed for recording the positive returns strokes discussed above. The negative return strokes (41 first strokes and 75 subsequent) occurred at distances ranging from 4 to 35 km (versus 7.8 to 157 km for the 48 positive strokes) from the field measuring station and had NLDN estimated peak currents ranging from 4.7 to 154 kA (versus 19.8 to 238 kA for the 48 positive strokes). The dependence of the NLDN-estimated peak current on distance for this sample of negative return strokes is rather weak (determination coefficient = 0.32). However, there is a bias toward larger peak currents, which increases with increasing distance. Table III gives the number of recorded strokes in different distance ranges along with the GM NLDN-estimated peak current for each distance range.

The scatter plot of the NLDN-estimated peak current I_{NLDN} versus electric field peak normalized to 100 km E for 116 negative return strokes is shown in Figure 5. The two parameters are linearly correlated (determination coefficient = 0.95), the relationship being given by the following regression equation:

$$I_{NLDN} = 2.29 - 3.06E \quad (5)$$

where E is positive and in V/m and I_{NLDN} is negative and in kA. The intercept (2.29) and slope (-3.06) in Equation 5 can be compared to those of Equation 3 (regression equation for 48 positive return strokes examined in this study) and to those of Equation 4 for D = 100 (regression equation of Rakov et al. (1992b) [9] for negative rocket-triggered lightning strokes). The values of corresponding regression equation parameters are similar. The variation in the parameters may be due to physical differences between natural negative return strokes (Equation 5), negative rocket-triggered lightning strokes (Equation 4), and natural positive return strokes (Equation 3) or due to smaller sample sizes for Equations 3 and 4. Figure 6 shows the scatter plot of the NLDN-estimated peak current versus measured electric field for all strokes combined (a total of 164 return strokes, of which 48 are positive and 116 are negative). The combined regression equation is given by:

$$I_{NLDN} = 7.81 - 3.58E \quad (6)$$

where E is positive for negative strokes and negative for positive ones and in V/m, and I_{NLDN} is negative for negative strokes and positive for positive ones and in kA.

It is important to note that the NLDN field-to-current conversion algorithm (discussed in Section III B) has been calibrated against direct current measurements only for negative subsequent strokes, with the median peak current estimation error being about 13% (Nag et al., 2011) [7]. Interestingly, there appears to be not much difference between first and subsequent strokes in Figures 3 and 5. In fact, the slopes in regression equations for negative first strokes and negative subsequent strokes given in Figure 5b are almost the same. This observation suggests that the NLDN procedure to compensate for field propagation effects and find the average range-normalized signal strength (RNSS) works equally for both subsequent and first return strokes.

D. Peak Currents Inferred from Measured Electric Field Peaks Using the Transmission Line Model

In this Section, we use the transmission line model (Uman and McLain, 1969 [2]) to infer peak currents from measured electric field peaks, NLDN reported distances, and assumed return-stroke speed. The relationship between the magnitudes of return-stroke peak current, I, and electric field peak, E, measured at distance D, based on the transmission line model, is given by (Rakov and Uman, 2003 [8], Chapter 4)

TABLE III. NUMBER OF NEGATIVE RETURN STROKES (41 FIRST AND 75 SUBSEQUENT) IN DIFFERENT DISTANCE RANGES AND CORRESPONDING GM NLDN-ESTIMATED PEAK CURRENTS.

Distance range, km	**5-10**	**10-20**	**20-30**	**30-40**	**0-40**
Number of events	26	80	3	7	116
GM NLDN-estimated peak current, kA	14	19	15	57	19

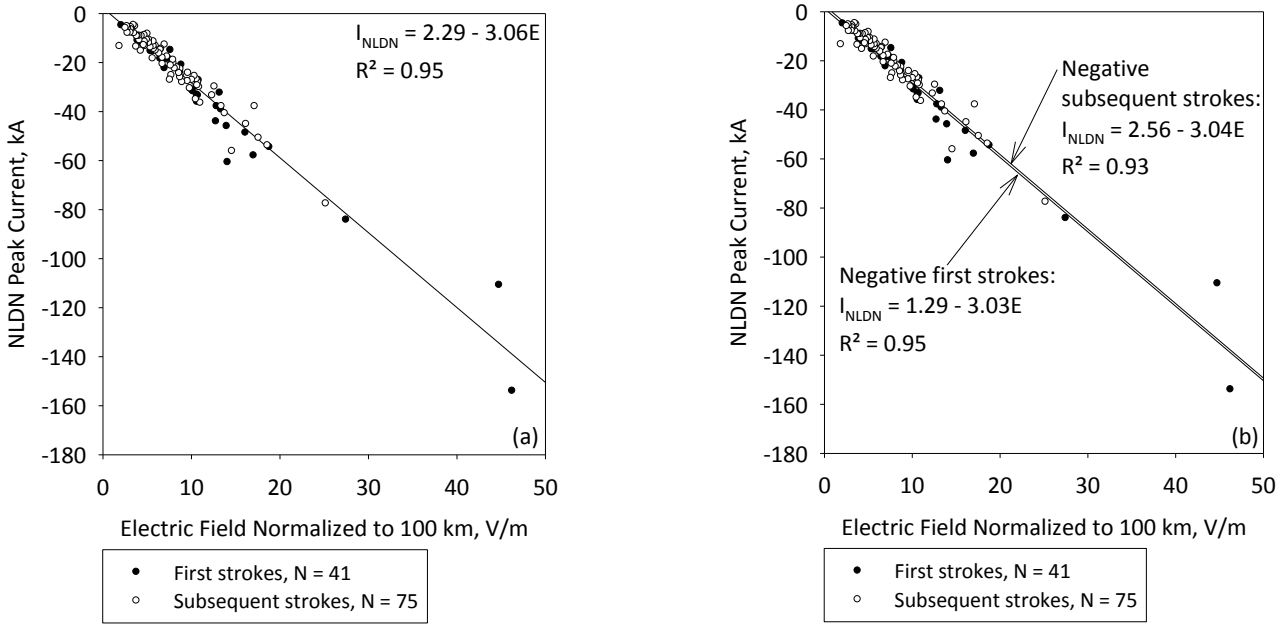

Figure 5. (a) NLDN-estimated peak current versus distance-normalized electric field peak for 116 first and subsequent negative return strokes. Also shown is the regression line. (b) Same as in (a) but with individual regression lines for 41 first and 75 subsequent strokes.

$$E = \frac{v}{2\pi\varepsilon_0 c^2 D} I \tag{7}$$

where ε_o is the permittivity of free space, c is the speed of light, and v is the return stroke speed.

Figure 7 shows scatter plots for the NLDN estimated peak current magnitudes versus magnitudes of peak currents estimated (for different values of v) using Equation 7 for 75 negative subsequent return strokes. Return-stroke speeds were assumed to be 10^8 m/s (Figure 7a), 1.5 x 10^8 m/s (Figure 7b), 1.8 x 10^8 m/s (Figure 7c), and 3 x 10^8 m/s (Figure 7d). The slanted line (slope = 1) is the locus of points for which the transmission line model estimated peak current and the NLDN-reported peak current are equal. It can be seen that the overwhelming majority of the points are above this line for v =10^8 m/s and v = 1.5 x 10^8 m/s, and below it for v = 3 x 10^8 m/s. For v = 1.8 x 10^8 m/s the points are found to be scattered more or less evenly around the line. Thus, it appears that the NLDN-reported peak currents are equal to the transmission line model predicted peak currents (for the 75 negative subsequent return strokes) for an assumed return stroke speed of 1.8 x 10^8 m/s. This suggests that the implied return-stroke speed in the NLDN field-to-current conversion equation is 1.8 x 10^8 m/s, provided that the NLDN measured field peak is consistent with ours.

The NLDN uses the same field-to-current conversion procedure (and hence the same implied return-stroke speed) for negative first strokes and positive return strokes as it does for negative subsequent strokes. We now check if there is a good match between NLDN-reported currents and transmission line model predicted currents for v = 1.8 x 10^8 m/s for negative first strokes and positive return strokes as well. Figures 8a and b show scatter plots of the NLDN-reported peak current versus the corresponding peak current estimated using Equation 7 for a return stroke speed of 1.8 x 10^8 m/s, for 41 negative first return strokes discussed in Section III C and the 48 positive return strokes presented in Section III B, respectively. The solid slanted line (slope = 1) in both plots is the locus of points for which the transmission line model estimated peak current and the NLDN-reported peak current are equal. One can see from Figure 8a that for the 41 negative first return strokes the NLDN-reported peak currents tend to be equal to the transmission line model predicted peak currents for the assumed return stroke speed of 1.8 x 10^8 m/s. However, for positive return strokes (Figure 8b) most data points are above

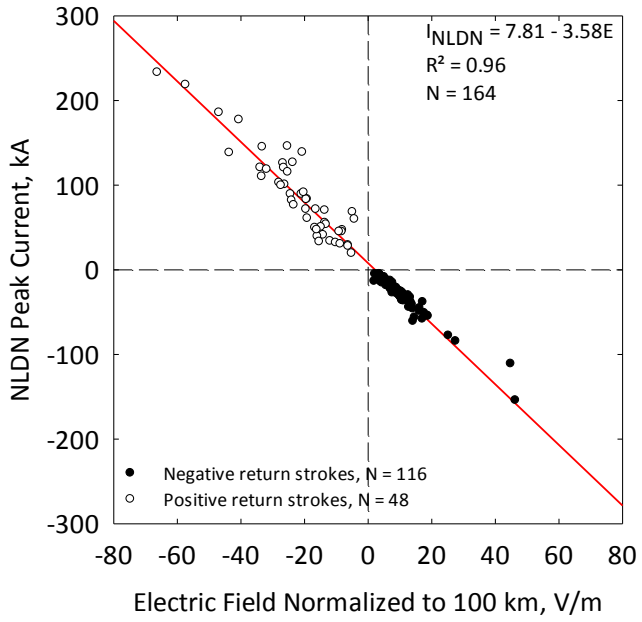

Figure 6. NLDN-estimated peak current versus measured electric field peak for 48 positive and 116 negative return strokes.

the diagonal (slope = 1 line). The relationship between the NLDN-reported peak current and the transmission line model estimated peak current for positive return strokes is given by the following regression equation:

$$\left| I_{NLDN} \right| = 11.3 + 1.27 \left| I_{TL} \right| \quad (8)$$

where I_{NLDN} and I_{TL} are in kA. For comparison, a similar regression equation for negative first and subsequent strokes for an assumed return stroke speed of 1.8 x 10^8 m/s is:

$$\left| I_{NLDN} \right| = -2.29 + 1.10 \left| I_{TL} \right| \quad (9)$$

where I_{NLDN} and I_{TL} are in kA. Note that Equation 8 can be derived from Equation 3 by using E = 0.36 I_{TL} (I_{TL} being positive and in kA and E being negative and in V/m), which is the relationship between electric field and current for the transmission line model for v = 1.8 x 10^8 m/s. Similarly, Equation 9 can be derived from Equation 5 using the same relation between E and I_{TL} (I_{TL} being negative and in kA and E being positive and in V/m).

IV. Discussion

For positive return strokes and an assumed return stroke speed of 1.8 x 10^8 m/s, NLDN-reported peak currents appreciably differ (by 27% on average) from the transmission line model predicted peak currents, as seen in Figure 8b and Equation 8. However, for negative return strokes and an assumed return stroke speed of 1.8 x 10^8 m/s, NLDN-reported peak currents are similar to (10% difference on average) the transmission line model predicted peak currents as seen in Figure 8a and Equation 9. We now examine the possible reasons of the discrepancy between negative first and subsequent strokes on the one hand and positive return strokes on the other hand.

One of the factors that may cause this discrepancy between positive and negative strokes is the limited bandwidth (400 Hz to 400 kHz) of the NLDN affecting the positive and negative strokes differently. We filtered our 48 electric field waveforms using a digital filter having a passband of 400 Hz to 400 kHz and a step response matching that of an NLDN sensor. The result of filtering for one positive return stroke is illustrated in Figure 9, which shows that the waveform after filtering becomes smoother and the peak value decreases (from 54 to 50 V/m). Histogram of the ratio of peaks in measured and filtered waveforms for the 48 positive return strokes is shown in Figure 10. The geometric mean ratio is 1.07 (meaning that the initial return stroke electric field peak decreases by 7% on average after filtering). For 44 negative return strokes mostly occurring at distances of a few hundred kilometers from the LOG, Haddad et al. (2012) [12] reported that the initial return stroke peak was found to decrease by 4.8% on average due to lowpass filtering with a 4-pole Bessel filter having -6-dB frequency of 400 kHz. So it seems that while the NLDN sensor bandwidth does decrease the peak value of the measured field, its effect on positive and negative strokes is not much different.

In order to study this discrepancy further, we examine the relative effect of propagation over lossy ground on field peaks of positive and negative return strokes. As stated in Section III B contributions from NLDN sensors at distances up to several hundreds of kilometers are included in calculation of peak currents. NLDN data from a storm occurring near the LOG on May 24, 2012 were used for this analysis. The NLDN recorded 1333 return strokes that occurred within 70 km of the measurement site. Of these strokes, 24 were positive with NLDN-estimated peak currents greater than 35 kA (selected to match the sample of 48 positive return strokes in this study), and 858 were negative with NLDN-estimated peak currents greater than 10 kA. For the 11 NLDN sensors within 625 km of the measurement site, these strokes were associated with 147 positive stroke sensor reports and 4403 negative stroke sensor reports. For each sensor report associated with a stroke, a relative gain was computed as the ratio of the sensor's peak current estimate to the NLDN-reported peak current determined as the average for all sensor reports within 625 km of the stroke location.

The average relative gain as a function of range from the measurement site (in 50 km bins) is shown in Figure 11 (top part). Positive and negative averages are shown separately. There is a clear upward trend in relative gain with increasing range, and there is little difference for positive and negative strokes. There is also a clear and common (for both positive and negative strokes) variation around this trend. It is important to note that since the strokes occurred within a small area (70 km radius); the relative gain at a specific range will be dominated by 1-2 sensors located at that distance from the stroke location. Since the NLDN sensors employ calibrated magnetic field measurements that are insensitive to local boundary conditions (such as those introduced by presence of

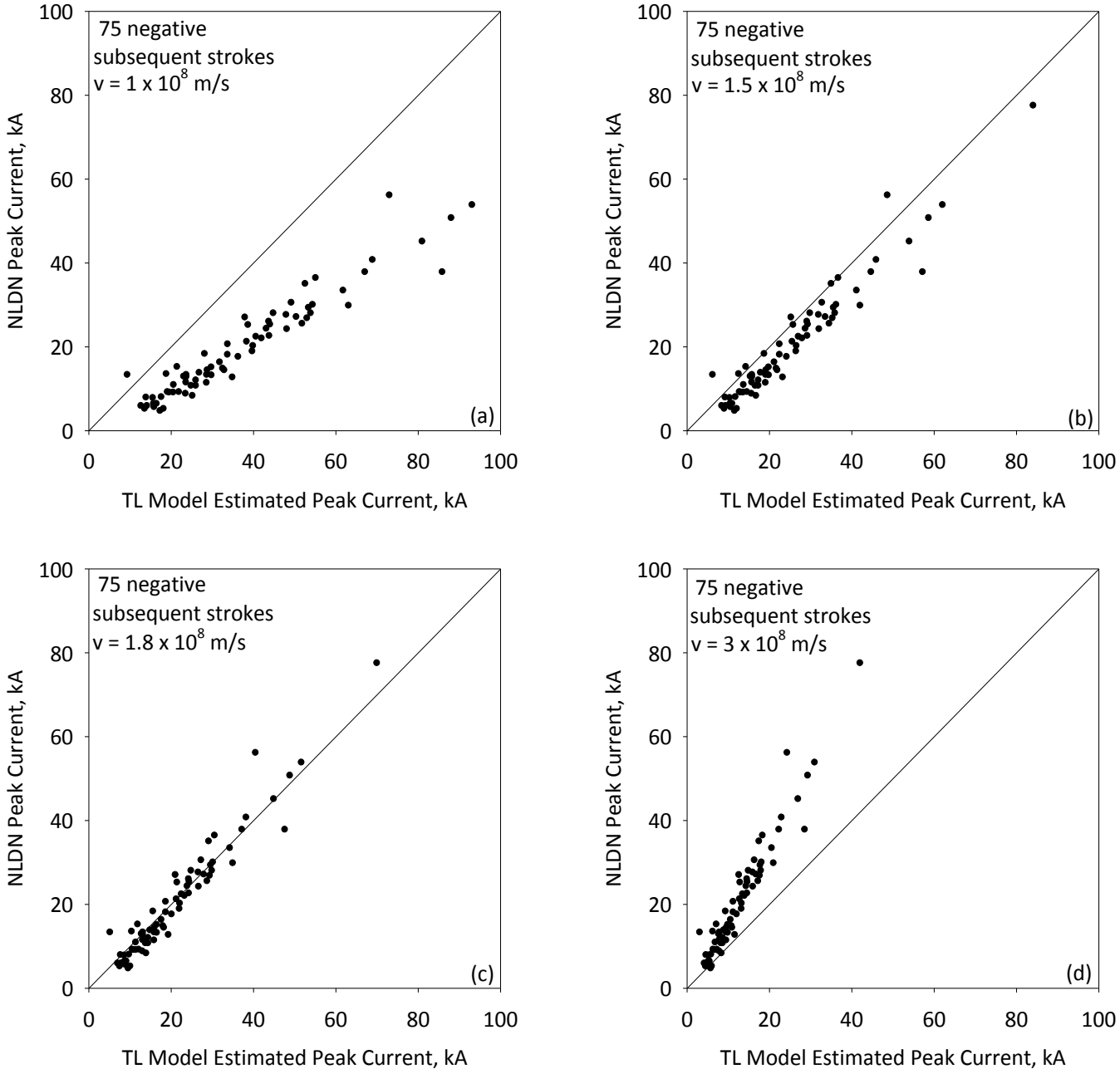

Figure 7. The NLDN-estimated peak currents versus peak currents estimated using the transmission line model for assumed return-stroke speeds of (a) 10^8 m/s, (b) 1.5 x 10^8 m/s, (c) 1.8 x 10^8 m/s, and (d) 3 x 10^8 m/s for 75 negative subsequent return strokes. Only the magnitudes of peak currents are considered.

structures near measurement site and local ground conductivity) the dominant sources of this range variation will be (1) directionally-dependent gain errors associated with local site-errors (Schulz and Diendorfer, 2002 [13]), and (2) variations in the path-averaged electrical conductivity between the stroke locations and each sensor. The underlying trend (~18% change over 600 km) is a result of a modest local bias in the space constant used in the NLDN propagation model (1000 km, Cummins et al., 2006 [6]). This value was selected to minimize the gain error, averaged throughout the whole U.S. Based on the findings shown here, the space constant "over corrects" for propagation in this region. In order to eliminate this bias in this dataset, the space constant had to be increased from 1000 to 1400 km (results are not shown here).

Figure 11 (bottom part) shows the histogram of the percentage of sensor reports in each 50 km range bin. The most probable range for the negative stroke reports is 300 km (18%), with very few reports above 500 km. For positive stroke reports, the most probable range in 550 km (17%), with lower and nearly-equal probability at all other ranges between 50 and 500 km. This indicates that there is a clear tendency for

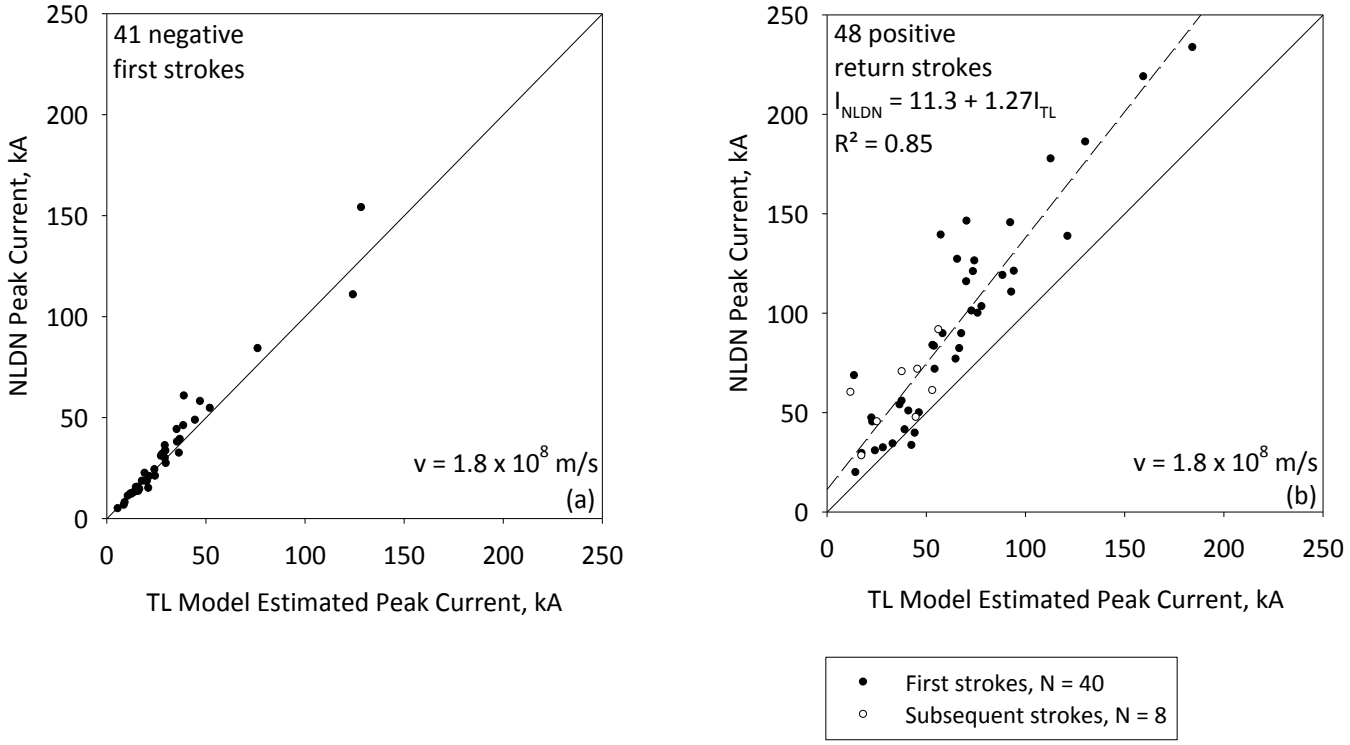

Figure 8. The NLDN-estimated peak currents versus peak currents estimated using the transmission line model for assumed return-stroke speed of 1.8 x 10^8 m/s for (a) 41 negative first return strokes and (b) 48 positive return strokes. Only the magnitudes of peak currents are considered.

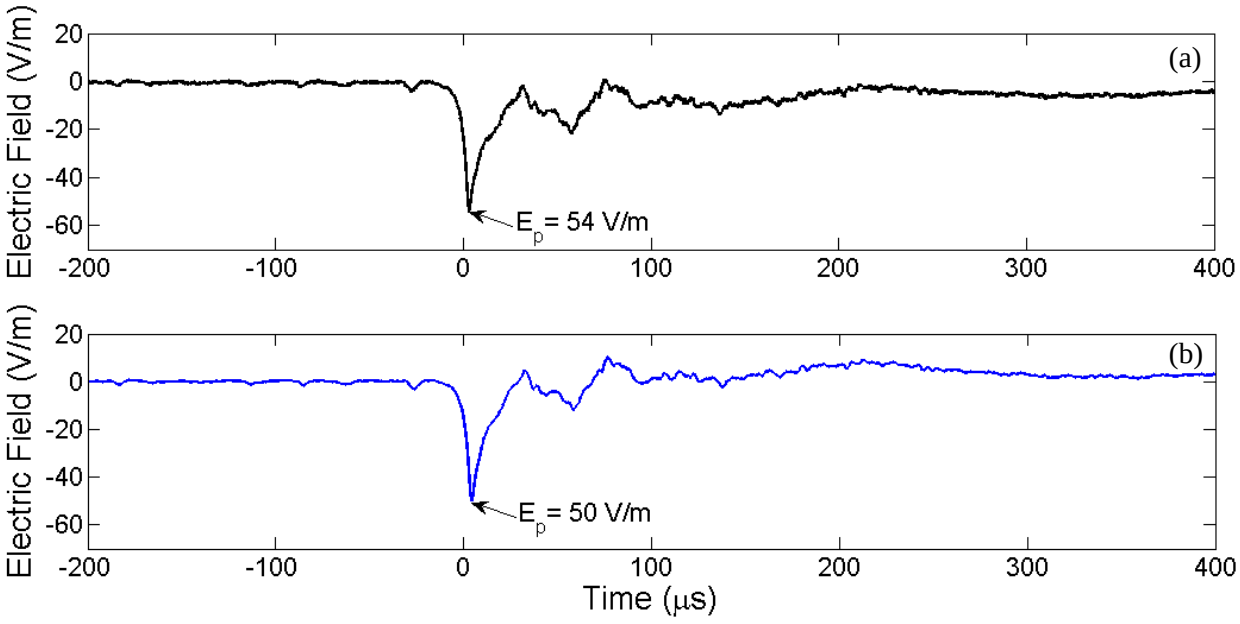

Figure 9. Positive return stroke electric field waveforms (a) before and (b) after applying 400 Hz to 400 kHz bandpass filter. The filtering simulates the bandwidth of the NLDN. Note that after filtering, the electric field peak E_p reduces from 54 to 50 V/m.

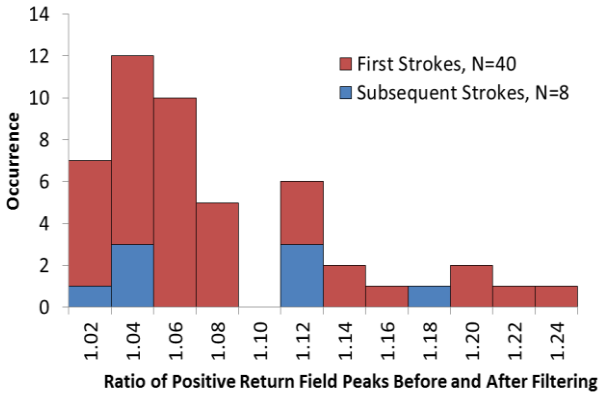

Figure 10. Histogram of the ratio of peaks in field waveforms before and after filtering for the 48 positive return strokes.

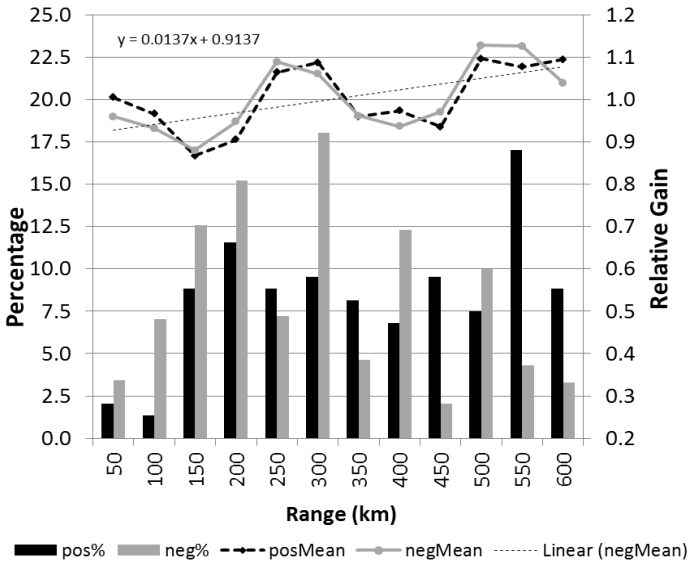

Figure 11. Average relative gain (right vertical axis) as a function of range from the measurement site in 50 km bins is shown at the top. The bottom part of the Figure shows histogram of the percentage of sensor reports (left vertical axis) in each 50 km range bin for positive and negative strokes.

positive strokes to be reported by sensors that are farther away because of their larger (than negative first strokes on average, Rakov and Uman, 2003 [8], Chapter 5) peak fields.

The combination of the bias towards NLDN sensor-reports from larger distances for positive strokes and the higher relative sensor gain at larger distances serve to produce on average 27% (see Figure 8b) higher peak current estimates for positive strokes in this region. This problem could be mitigated using a propagation correction for amplitude effects in the NLDN, similar to that used to reduce time-of-arrival errors and hence improve location accuracy (Cummins et al., 2010 [14]).

V. Concluding Remarks

We recorded 48 positive strokes in 40 flashes that were correctly identified by the NLDN and located at distances ranging from 7.8 to 157 km from the Lightning Observatory in Gainesville (LOG), Florida. We examined peak currents inferred from radiation electric field peaks of these 48 positive return strokes and compared them to the corresponding NLDN-reported peak currents.

Using the radiation-field-to-current relationship based on the transmission line model we estimated the return-stroke speed implicitly used in the NLDN field-to-current conversion equation to be 1.8 x 10^8 m/s. This value of speed appears to work equally well for both first and subsequent negative strokes, but not for positive strokes. The difference can be explained by the bias towards NLDN sensor reports from larger distances for positive strokes combined with the higher relative sensor gain at larger distances. This problem could be mitigated using a propagation correction for amplitude effects in the NLDN, similar to that used to reduce time-of-arrival errors and hence improve location accuracy (Cummins et al., 2010 [14]).

References

[1] A. Nag and V. A. Rakov (2012), "Positive lightning: An overview, new observations, and inferences," J. Geophys. Res., 117, D08109, doi:10.1029/2012JD017545.

[2] M. A. Uman and D. K. McLain, "Magnetic field of the lightning return stroke," J. Geophys. Res., 74, 6899–6910, 1969.

[3] A. Nag, "Characterization and modeling of lightning processes with emphasis on compact intracloud discharges," PhD dissertation, Univ. of Fla., Gainesville, 2010.

[4] A. Nag, V. A. Rakov, D. Tsalikis, and J. A. Cramer, "On phenomenology of compact intracloud lightning discharges," J. Geophys. Res., 115, D14115, doi:10.1029/2009JD012957, 2010.

[5] Y. Baba and V. A. Rakov, "Electromagnetic fields at the top of a tall building associated with nearby lightning return strokes," IEEE Trans. Electromagn. Compat., 49(3), 632–643, doi:10.1109/TEMC.2007.902402, 2007.

[6] K. L. Cummins, J. A. Cramer, C. Biagi, E. P. Krider, J. Jerauld, M. A. Uman, and V. A. Rakov, "The U.S. National Lightning Detection Network: Post-upgrade status," paper 6.1 presented at the Second Conference on Meteorological Applications of Lightning Data, Am. Meteorol. Soc., Atlanta, Ga., 2006.

[7] A. Nag, S. Mallick, V.A. Rakov, J. Howard, C.J. Biagi, D. Hill, M.A. Uman, D.M. Jordan, K.J. Rambo, J. Jerauld, B.A. DeCarlo, K.L. Cummins, and J.A. Cramer, "Evaluation of NLDN performance characteristics using rocket-triggered lightning data acquired in 2004–2009," Journal of Geophysical Research, 116, D02123, doi:10.1029/2010JD014929, 2011.

[8] V. A. Rakov and M. A. Uman, Lightning: Physics and Effects, Cambridge Univ. Press, New York, 2003.

[9] V. A. Rakov, R. Thottappillil, and M. A. Uman, "On the empirical formula of Willett et al. relating lightning return-stroke peak current and peak electric field," J. Geophys. Res., 97(D11), 11,527–11,533, 1992b.

[10] J. C. Willett, J. C. Bailey, V. P. Idone, A. Eybert-Berard, and L. Barret, "Submicrosecond intercomparison of radiation fields and currents in triggered lightning return strokes based on the transmission-line model," J. Geophys. Res., 94, 13,275–13,286, 1989.

[11] A. Pavlick, D. E. Crawford, and V. A. Rakov, "Characteristics of distant lightning electric fields," paper presented at 7th International Conference on Probabilistic Methods Applied to

Power Systems, Assoc. per gli Studi sulla Qualita dell 'Energia Elet., Naples, Italy, 2002.

[12] M. A. Haddad, V. A. Rakov, and S. A. Cummer, "New measurements of lightning electric fields in Florida: Waveform characteristics, interaction with the ionosphere, and peak current estimates," J. Geophys. Res., 117, D10101, doi:10.1029/2011JD017196, 2012.

[13] W. Schulz and G. Diendorfer, "Amplitude site error of magnetic direction finder," 26th International Conference on Lightning Protection, Cracow, Poland, September 2-6, 2002.

[14] K. L. Cummins, M.J. Murphy, J.A. Cramer, W. Scheftic, N. Demetriades, A. Nag, "Location accuracy improvements using propagation corrections: A case study of the U.S. National Lightning Detection Network," 21st International Lightning Detection Conference, Orlando, April, 2010.